



OPEN Distribution, environmental risks, and conservation challenges of chemical pollutants in Persian Gulf marine protected areas

Maryam Ghaemi¹✉, Farshid Soleimani^{1,2}, Hossein Arfaeinia³ & Sara Gholamipour¹

This study investigates the occurrence and distribution of chemical pollutants, including total petroleum hydrocarbons (TPHs), organochlorine pesticides (OCPs), polychlorinated biphenyls (PCBs), anionic surfactants, and total organic carbon (TOC), in the Marine Protected Areas (MPAs) waters in the northern Persian Gulf. Water samples were collected from five MPAs during the winter and summer of 2022. The study identified significant seasonal variations, with higher pollutant levels recorded in winter compared to summer. Concentrations of Σ 19PCBs (ng/L), anionic surfactants (μ g/L), TPHs (mg/L), and TOC (mg/L) ranged from 0.72 to 4.66, 10 to 79, ND to 134.63, and 0.5 to 114.58 in winter, and from 2.49 to 5.05, 11 to 30, ND to 20.26, and 0.15 to 5.27 in summer, respectively. The pollution patterns revealed the Mond protected area as a major pollution hotspot, compromising its ecological health. The results highlight the critical need for targeted pollution control and enhanced conservation measures in the region's MPAs to protect biodiversity and marine ecosystems.

Keywords Marine pollution, Marine protected area, Persian Gulf, Risk assessment

In recent years, the expansion of industrial activities, urbanization, population growth, and the widespread use of fertilizers and pesticides have significantly increased water pollution^{1–3}. Approximately 80% of marine pollution originates from land-based sources, primarily from nonpoint sources such as agricultural runoff. Sea-based activities, including shipping, seabed mining, mariculture, antifouling biocides, dredging, and dumping, also contribute significantly to the release of pollutants into marine environments⁴. Water pollutions can be classified as organic and inorganic pollutants, microbial agents, suspended solids, nutrients, thermal pollution, radioactive materials, and other pollutants, often discharged through sewage, agricultural runoff, and industrial effluents⁵.

Marine and coastal ecosystems provide food, pharmaceuticals, building materials, revenue, and jobs in various sectors such as fisheries and tourism^{6,7}. These ecosystems also offer a range of services, such as shoreline stabilization, protection against extreme weather events like storms and floods, pollutant processing, and serving as nurseries for fish and other species. Furthermore, marine ecosystems play a crucial role in climate regulation, nutrient cycling, and productivity^{6–8}.

However, human activities are placing increasing pressure on ecologically valuable coastal zones, often with synergistic effects that compound their impact on biodiversity and ecosystem health^{7,9,10}.

The Persian Gulf (PG), a semi-enclosed water body connected to the Indian Ocean via the Strait of Hormuz¹¹, faces severe environmental stress due to heavy industrialization, shipping, and pollution^{12–14}. Major river inflows, including the Arvand (Shatt Al-Arab), Hendijan, Helleh, and Mond rivers, primarily located on the Iranian side, contribute to pollution in the northern Gulf¹⁵. The Persian Gulf is home to diverse marine life but remains highly vulnerable to persistent pollutants like total petroleum hydrocarbons (TPHs), organochlorine pesticides (OCPs), polychlorinated biphenyls (PCBs), and anionic surfactants, which pose long-term ecological risks due to their persistence and bioaccumulative nature^{12,13,16,17}.

Marine Protected Areas (MPAs) have been established to safeguard these ecosystems by regulating human activities¹⁸. While MPAs are critical for marine biodiversity management, many are located near pollution sources, such as ports, industrial sites, agricultural runoff, and urban areas, making them vulnerable to chemical

¹Iranian National Institute for Oceanography and Atmospheric Science, No. 3, Etemadzadeh St., Fatemi Ave., Tehran 1411813389, Iran. ²Tobacco and Health Research Center, Hormozgan University of Medical Sciences, Bandar Abbas, Iran. ³Department of Environmental Health Engineering, Faculty of Health, Bushehr University of Medical Sciences, Bushehr, Iran. ✉email: mghaemi@inio.ac.ir; maryam.ghaemi@gmail.com

contamination^{18–22}. Research suggests that MPA designation alone may not be sufficient to prevent pollution-related damage²³.

Despite their importance, there is limited research on the chemical contamination of MPAs, particularly in the Persian Gulf. Persistent organic pollutants like TPHs, OCPs, PCBs, and anionic surfactants present serious risks to these sensitive environments. Monitoring these contaminants is essential to assess pollution levels, identify sources, and evaluate the health of MPAs in the region.

This study fills a critical knowledge gap by providing the first comprehensive assessment of chemical pollution in MPAs across the northern Persian Gulf. The research focuses on both spatial and seasonal variations in pollutant levels, offering essential baseline data for future conservation efforts. By identifying pollution hotspots and analyzing the sources of contamination, this study enhances our understanding of MPA effectiveness and underscores the urgent need for stronger management strategies to protect these vulnerable ecosystems.

Materials and methods

Study area and sampling

Seawater samples were collected from Marine Protected Areas (MPAs) in the northern Persian Gulf, specifically in Bushehr Province, Iran. The sampling locations included the Mond Protected Area (stations M1, M2, and M3), Helleh Protected Area (stations H1 and H2), Nakhiloo National Park (stations NL1 and NL2), Nayband National Park (stations NB1 and NB2), and Khark Coral Island, totaling 10 stations. The locations of these stations are shown in Fig. 1. Basic information about the sampling stations, including latitude, longitude, surface water temperature, salinity, percent saturation of dissolved oxygen (%DO), conductivity, and pH, is provided in Table 1. Water samples were collected in triplicates (at different stations) during both the winter (January–February 2022) and summer (June 2022) seasons.

At each station, a water sample was collected from a depth of 1 m using a 10-liter Niskin bottle sampler (Hydro-Bios, Kiel, Germany), ensuring no contamination from the boat. Subsamples were taken immediately for the analysis of TPHs, anionic surfactants, TOC, OCPs, and PCBs. TOC and anionic surfactant subsamples were placed in pre-cleaned high-density polyethylene bottles, while TPHs, OCPs, PCBs, and anionic surfactant samples were collected in pre-cleaned amber glass bottles. TOC and TPH samples were promptly acidified with 50% sulfuric acid (H_2SO_4) and 6 mol/L hydrochloric acid (HCl) to reduce the pH to below 2. All samples were preserved right after collection by storing them in ice chests at 4 °C until further processing and analysis.

Water samples analysis

During sampling, physicochemical parameters such as pH, surface water temperature, salinity, dissolved oxygen, and conductivity were measured at each location using a HACH portable meter HQ40d. Seawater temperature and pH were measured using a combined glass/reference electrode (HACH, IntelliCAL PHC101),

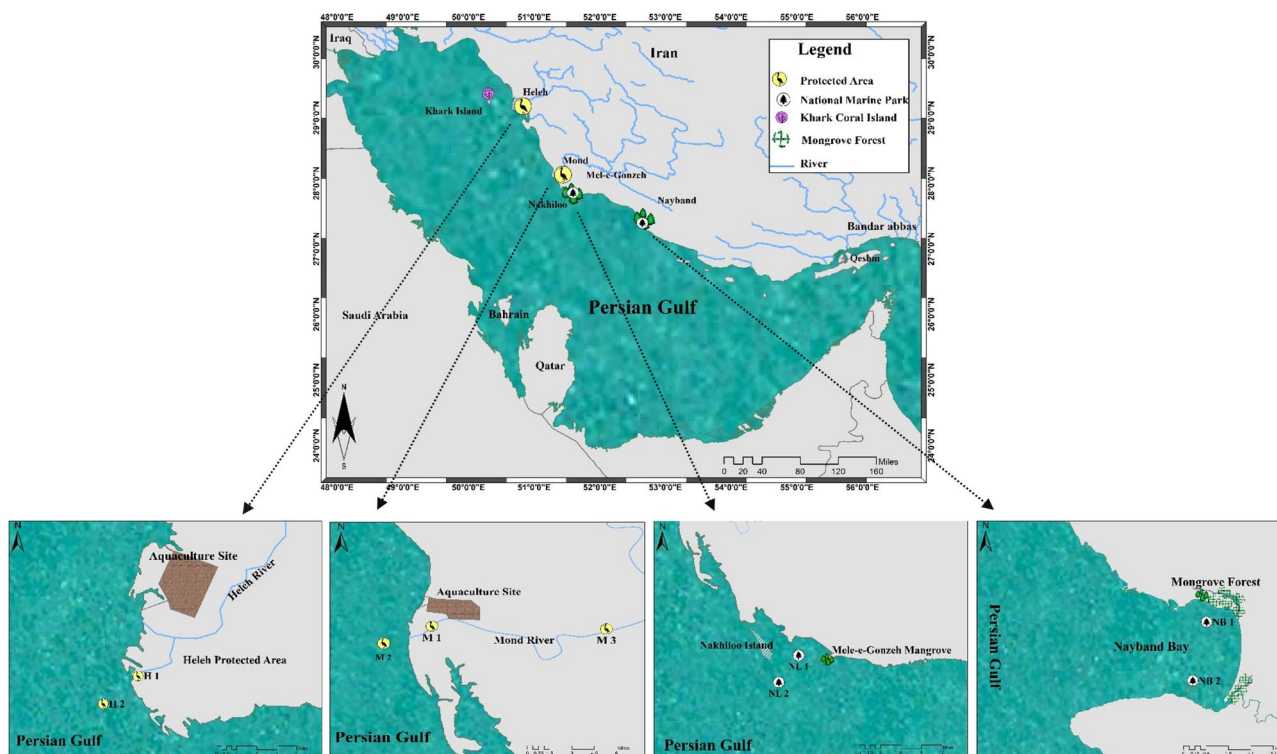


Fig. 1. The location of study stations within the marine protected areas that are spread across the northern Persian Gulf, Bushehr province, Iran. The map was created using Esri ArcMap, version 10.3 (available at <https://desktop.arcgis.com/en/arcmap/10.0/>).

Stations	Lat.	Long.	T (°C)		Sal.		Con. (mS/cm)		pH		%DO	
			Summer	Winter	Summer	Winter	Summer	Winter	Summer	Winter	Summer	Winter
NB1	27.446023	52.656113	34.5	17.3	37.3	38.7	49.3	51.2	8.2	8.1	125.4	121.0
NB2	27.411862	52.64812	34.2	21.6	38.2	38.1	50.2	51.2	8.2	8.1	127.2	130.3
H1	29.144895	50.64383	28.9	11.6	41.3	3.9	54.2	5.5	8.1	7.9	122.3	98.0
H2	29.133812	50.633921	30.2	11.2	40.5	38.3	53.2	52.3	8.2	8.1	126.0	132.4
M1	28.15305	51.291272	31.2	17.5	40.3	15.3	52.7	22.8	8.2	7.8	131.2	102.0
M2	28.131163	51.245469	30.1	20.6	39.3	38.0	51.7	49.8	8.2	8.1	126.6	123.8
M3	28.149956	51.461137	34.4	16.4	67.0	1.8	82.0	3.3	8.1	7.9	163.1	98.1
NL1	27.851254	51.522387	32.4	21.2	49.9	39.1	49.9	52.2	8.2	8.1	130.2	130.1
NL2	27.792698	51.480302	32.0	22.4	49.9	39.1	49.9	52.1	8.2	8.1	131.4	130.1
Khark Island	29.277691	50.309405	32.8	19.9	38.8	40.5	51.0	53.9	8.2	8.2	129.9	128.3

Table 1. Basic information of sample stations.

calibrated with NBS buffers (accuracy of ± 0.02 , precision of ± 0.001). Dissolved oxygen levels were determined using a calibrated optical sensor (HACH, IntelliCAL LDO101 luminescent/optical dissolved oxygen probe). Conductivity and salinity were measured with a conductivity probe (HACH, IntelliCAL CDC401, with a precision of ± 0.1), calibrated with a certified reference seawater.

For measurement of pollutants at each station, separate subsamples were taken and analyzed using the respective standard methods appropriate for each parameter.

The concentration of anionic surfactants was determined using the Crystal Violet Method 8028. TOC levels were measured by high-temperature combustion using a TOC Analyzer (Shimadzu TOC-Vcsh), following standard method 5310B. Carbon dioxide was purged out of the acidified samples by bubbling N₂ gas before the TOC content was determined following the high temperature (680 °C) catalytic oxidation method, using an Apollo 9000 TOC Analyzer with an NDIR detector (Teledyne Tekmar, Ohio, USA). Certified reference material procured from Analytik Jena was used for calibration before each set of measurements. Another TOC standard (1 mg C/L) and a blank (milli Q water) were run after each set of samples, and sometimes in between the samples, to check the performance of the instrument. In case of a shift in the area unit value relative to the initial calibration, appropriate correction was made.

To extract TPHs from water samples, the MOOPAM standard (1999) was employed. After spiking each sample with a surrogate standard (p-Terphenyl-D14), water samples (1000 mL) were extracted three times using a separatory funnel with 50 mL portions of n-hexane. The extracts were concentrated to a volume of 1 mL. The concentrations of saturated (aliphatic) hydrocarbons or TPHs (C10 -C40, Pristane and Phytane) were analyzed using an Agilent 6890 N gas chromatograph equipped with an HP-5 capillary column (30 m in length, 0.25 mm in diameter, and 0.25 μ m film thickness). One microliter of the extract was injected in splitless mode at 280 °C with a total flow rate of 1 mL/min. The oven temperature was initially set at 50 °C for 5 min, then ramped at a rate of 10 °C/min until reaching 300 °C (20 min). A five-point serial dilution of calibration standards (2.00, 6.00, 10.00, 50.00, and 100.00 mg/L) was prepared from the stock solution and used to calibrate the GC-MS before analysis. After calibration, the samples were analyzed, and the concentrations were calculated accordingly.

For the extraction of OCPs and PCBs from water samples, EPA methods 608 and 3510 C (separatory funnel liquid-liquid extraction) were used, respectively. Water samples (1000 mL) were extracted three times using a separatory funnel with 50 mL portions of dichloromethane solvent, after spiking with surrogate standards (p-Terphenyl-D14 for OCPs and PCB209 for PCBs). The extracts were concentrated to 1 mL. OCPs and PCBs were analyzed separately with an Agilent 6890 N Series GC System connected to an Agilent 5973 Network Mass Selective Detector. Separation was accomplished with a HP-5 capillary column (30 m \times 0.25 mm i.d., 0.25 μ m film thickness). Samples (1 μ L) were injected in splitless mode. For OCPs, the column flow was maintained at 1.0 mL/min with the following temperature program: initial oven temperature of 100 °C (2 min), ramping at a rate of 15 °C/min to 160 °C (5 min), and finally to 280 °C (5 min) at 5 °C/min. The injection port temperature was maintained at 270 °C. PCBs were analyzed with the following temperature program: initial oven temperature of 130 °C (2 min), then ramped at a rate of 15 °C/min to 160 °C, and finally at 5 °C/min to a final temperature of 300 °C with a final holding time of 6 min with the same flow rate and injector port temperature as the OCP method. OCPs and PCBs quantification was accomplished through the application of a 5-point calibration curve by running a series of standards.

Strict quality control and assurance protocols were followed, including the analysis of procedural blanks and spiked samples with each batch. The recovery rates for OCPs, TPHs, and PCBs ranged from 75.7 to 119.8%, 82.1–105.6%, and 88.0–116.6%, respectively. The reproducibility of replicate measurements was within approximately 10% for OCPs and TPHs, and 12% for PCBs. Inter-laboratory assessments were also conducted on a number of samples to verify the methodology and results. The limit of detection (LOD) was consistent with a concentration which would give a signal/ noise ratio of 3. The LODs of OCPs and PCBs are listed in Tables S1 and S2, respectively.

Statistical analyses

The SPSS software (version 26) was used for statistical analysis of the data. ANOVA and Tukey Post Hoc tests were conducted to determine statistical differences between the stations and seasons. A p-value of < 0.05 was considered statistically significant. The maps were created using Esri ArcMap, version 10.3, which is available at <https://desktop.arcgis.com/en/arcmap/10.0/>.

Results and discussion

The measured physicochemical parameters and chemical pollutants in the seawater of the MPAs are detailed in Table 1; Figs. 2–7, respectively. The concentration ranges of TOC, TPHs, PCBs, DDTs, HCHs, OCPs, and anionic surfactants in Persian Gulf MPAs waters are compared to those collected from different coastal areas worldwide in Table 2.

Measurement of physicochemical parameters

The highest surface water temperature range was recorded in the summer of 2022, varying from 28.9 to 34.5 °C, while the lowest range, from 11.2 to 22.4 °C, was observed in the winter of 2022 (Table 1). The pH values ranged from 7.8 to 8.2 during winter and from 8.1 to 8.2 during summer (Table 1). Salinity, which influences the distribution and diversity of many marine species²⁴, varied widely, ranging from 1.8 to 40.5 in winter and 37.3 to 67.0 in summer (Table 1). The European Union Directive [79/923/EEC] considers a salinity range of 12–38 as an acceptable limit in coastal waters (Environmental Protection Agency, Ireland).

Figure 2, shows the spatial distribution of salinity across the study area in winter (right) and summer (left). The lowest salinity levels were recorded at 1.80 in station M3 (located in the Mond River) and 3.90 in station H1 (located at the mouth of the Helleh River) during the winter (rainy season). The decrease in salinity during

Compounds	Location	Sampling time	Concentrations		References
			Average	Range	
TOC (mg/L)	Northern PG, Iran	January–February and June 2022	7.48	0.15–114.58	This study
	Southern PG, UAE	April 1986	2.7	0.8–3.9	29
	Southern PG, Qatar	April 1986	1.6	0.5–3.6	30
	Southern PG and GO ¹	February–March, 1987	6.37	2.1–14.6	29
	Northern PG, Kuwait	March 2014–March 2016	1.93	1.21–3.82	31
	Northern Arabian Sea	1995–1996	–	0.96–1.2	37
	Indian, Pacific, and Atlantic Oceans	–	–	1.5–2.0	38
	Northern Coastal Baltic Sea	1975–2011	–	3–6	39
TPH (mg/L)	Northern PG, Iran	January–February and June 2022	15.71	nd–134.6	This study
	Ondo state, Nigeria	November 2017–April 2018	–	nd–4.07	40
	Teluk Batik Beach, Malaysia	July 2018	–	91–503	41
	Algoa Bay, Eastern Cape, South Africa	February to June 2016	0.118	0.045–0.273	42
	Tianjin Bohai Bay, China	1996–2005	0.096	0.020–0.508	43
HCHs (ng/L)	Northern PG, Iran	January–February and June 2022	39.56	nd–141.28	This study
	Lake Burullus, Egyptian Mediterranean Sea	2006	–	nd–495.55 ^a	44
	Near-shore surface water of Alexandria, Egypt	2013–2014	0.33	0.16–0.63	45
	Bohai Bay, north of China	–	160	50–750	35
	Daya Bay	August 1999	285	36–1229	46
	Northern South China Sea	2009–2011	2.57	0.23–20.02	47
	East China Sea	2009–2011	1.64	0.08–7.20	47
	Beibu Gulf, northwest of the South China Sea	May 2021	0.19	0.06–0.82	48
	North Atlantic Ocean	2015	–	0.09–0.63	49
	Minjiang River Estuary, China	November 1999	205.50	52.09–515.0	50
	Marginal seas of China	Sep–Oct 2006	1.29	0.68–2.04 ^b	51
	Bering Sea, Northern Pacific Ocean	July–Sep 1999	0.41	0.15–0.81	52
	Chukchi Sea, Arctic Ocean	July–Sep 1999	0.44	0.14–0.94	52
DDTs (ng/L)	Northern PG, Iran	January–February and June 2022	0.09	nd–1.71	This study
	Lake Burullus, Egyptian Mediterranean Sea	2006	–	0.07–882.6	44
	Near-shore surface water of Alexandria, Egypt	2013–2014	2.50	0.22–16.86	45
	Bohai Bay, north of China	–	–	10–110	53
	Daya Bay	August 1999	175	27–975	46
	China's surface water	–	0.5–175.0	nd–975.9	54
	Laguna de Terminos, Mexico	April 2000	0.28	0.07–0.60	55
	Northern South China Sea	2009 to 2011	0.97	0.0–15.16	47
	East China Sea	2009–2011	0.72	0.0–9.36	47
	Beibu Gulf, northwest of the South China Sea	May 2021	0.44	0.01–2.46	48
	Gulf of Milazzo (Southern Italy)	2005	1.6	0.60–6.89	56
	North Atlantic Ocean	2015	–	nd–0.002	49
	Minjiang River Estuary, China	November 1999	142.0	40.61–233.5	50
	Marginal seas of China	Sep–Oct 2006	1.27	0.52–2.57	51
	Bering Sea, Northern Pacific Ocean	July–Sep 1999	–	0.01–0.09	52
Chukchi Sea, Arctic Ocean	July–Sep 1999	–	0.05–0.12	52	
OCPs (ng/L)	Northern PG, Iran	January–February and June 2022	68.55	3.13–219.6	This study
	Beibu Gulf, northwest of the South China Sea	May 2021	0.85	0.12–2.81	48
	Gulf of Milazzo (Southern Italy)	2005	4.52	0.24–20.82	56
	Minjiang River Estuary, China	November 1999	839.9	214.4–1819	50
	Marginal seas of China	Sep–Oct 2006	2.93	1.45–5.23	51
Continued					

Compounds	Location	Sampling time	Concentrations		References
			Average	Range	
PCBs (ng/L)	Northern PG, Iran	January–February and June 2022	2.95	0.72–5.05	This study
	Shadegan Wetland, northwestern PG	–	93.25	8–375 ^c	57
	Larak Coral Island, PG	Winter and summer 2015	1.39	0.97–3.10	58
	Lake Burullus, Egyptian Mediterranean Sea	2006	1756.7	1.029–3315.8 ^c	44
	Near-shore surface water of Alexandria, Egypt	2013–2014	33.91	2.44–90.61	45
	Bohai Bay, north of China	–	–	60–700	53
	Bay of Bengal coast of Bangladesh	Winter and summer 2015	–	4.22–30.84 ^c	59
	Laguna de Terminos, Mexico	April 2000	1.18	0.07–3.40	55
	North Atlantic Ocean	2015	–	0.011–0.025 ^c	49
	Minjiang River Estuary, China	November 1999	985.2	203.9–2473	50
Anionic surfactant (µg/L)	Northern PG, Iran	January–February and June 2022	30.53	10–79	This study
	Black Sea coastline of Turkey	Autumn 2010–winter 2011	–	30–186	60
	Gdańsk Bay, southeastern part of the Baltic Sea	November 2001 to May 2002	–	5–150	61

Table 2. Comparison of chemical compound with other sea area in the world. a: Total HCHs concentrations including α -HCH, β -HCH, and lindane; b: Total HCHs concentrations including α -HCH and γ -HCH; c: PCB28, -52, -101, -118, -153, -138, -180; nd: below limit of detection; 1: GO, Gulf of Oman.

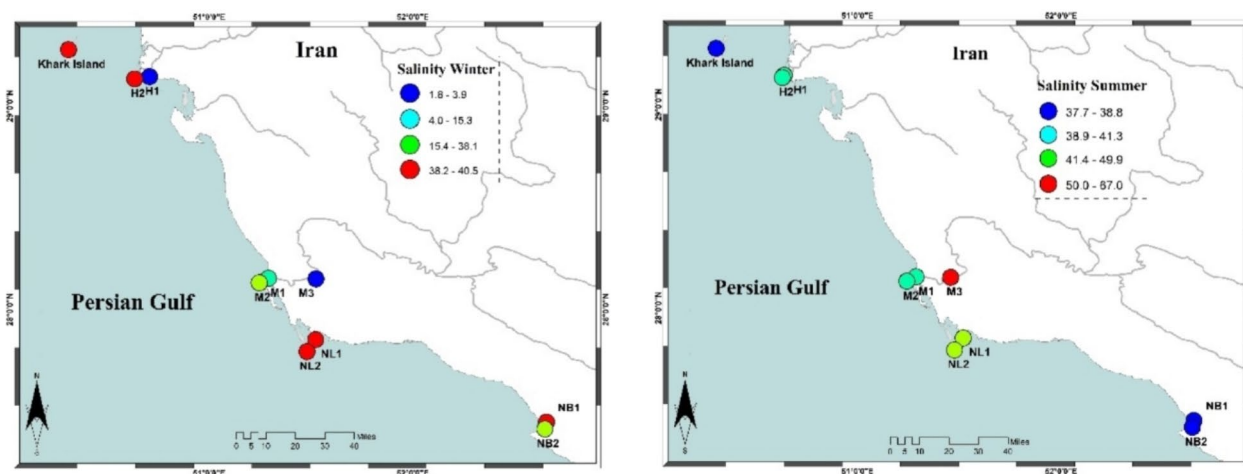


Fig. 2. The spatial distribution of salinity across the study area in winter (right) and summer (left). The map was created using Esri ArcMap, version 10.3 (available at <https://desktop.arcgis.com/en/arcmap/10.0/>).

winter, coupled with an increase in water depth (from 0.5 to 2 m at station M3 and from 1.5 to 2 m at station H1), reflects the significant freshwater influx resulting from the winter 2022 rainfall upstream of these rivers. According to the Iran Meteorological Organization (www.irimo.ir), the total rainfall from January 21 to February 19 (the sampling period) at Dayyer station was 186 mm, while the total rainfall during other months of 2022 was only 17.8 mm. The Dayyer station, located about 60 km from the Mond River estuary, is the nearest weather station to the study area. The nearest meteorological synoptic station to station H1 (Helleh River) is Bandar-e Rig, which recorded 105 mm of rainfall from January 21 to February 19, with a total rainfall of 9 mm during the rest of 2022. The highest salinity level (67.0) was observed at station M3 during the summer (dry season). The Mond River's salinity is unusually high for freshwater inputs due to its passage through areas with high salt content, particularly the Jashak Salt Dome (or Kuhe-Namakak) in Bushehr Province, Iran, which is the primary source of hypersaline water in the Mond River²⁵. The background salinity of the Mond River fluctuates between 5 and 20 during the wet season and between 40 and 50 during the dry season, depending on the influx of low-salinity riverine water or runoff from highly saline soils²⁶, unpublished data.

The Mond River, with its many branches, including the main branch Kara-Aghaj River, originates in Fars Province and flows into the Persian Gulf after entering Bushehr Province. This river, the fifth longest in Iran, is permanent and the most important and largest river in Bushehr Province, stretching 750 km. The Helleh River is formed by the confluence of the Dalaki and Shapur rivers, which originate in the Zagros Mountains and enter the Persian Gulf at the northern end of Bushehr city. Wetlands at the confluence, part of the Helleh protected area, are crucial for migrating birds.

Conductivity values ranged from 49.3 to 82.0 mS/cm in summer and from 3.3 to 53.9 mS/cm in winter. Although no specific guideline for conductivity is available, seawater values as high as 55 mS/cm are possible, depending on water temperature and salinity²⁷.

Dissolved oxygen saturation (%DO) levels ranged from 98.1 to 132.4% (equivalent to 8.9–11.4 mg/L) during winter, and from 122.3 to 163.1% (equivalent to 7.2–8.0 mg/L) in summer. Oxygen supersaturation (values exceeding 130%), which may indicate increased phytoplankton photosynthesis, was observed at station M3 in summer (Table 1). Oxygen supersaturation during the day may result in nighttime deoxygenation due to respiration in the absence of photosynthesis²⁸. Further investigation is required to confirm the actual oxygen status of these waters. However, the supersaturation level at station M3 (163.1%) is unlikely to cause hypoxic or anoxic conditions during the night. In the study by O'Boyle et al., supersaturation levels ranged from 132.8 to 162.4%²⁸. Diurnal variations in oxygen levels, commonly observed in nutrient-rich waters, suggest that relying solely on oxygen concentration may provide a misleading assessment of oxygen conditions. For instance, in the Broadmeadow Estuary (Irish waters), an oxygen concentration of 10.9 mg/L might indicate healthy conditions, but a corresponding saturation level of 139% suggests enhanced phytoplankton activity, potentially leading to nighttime oxygen depletion²⁸.

The environmental quality standards (EQSs) for dissolved oxygen in estuarine and coastal waters, as defined by the EU Water Framework Directive, are outlined in the EC Environmental Objectives (Surface Waters) Regulations S.I. 272 of 2009. These standards are based on oxygen saturation levels rather than concentration, with both lower and upper thresholds set for undersaturation and supersaturation. For instance, to comply with the EQS for dissolved oxygen in estuarine waters, 95% of the readings must show saturation levels between 70% and 130%.

TOC analysis

There is no prior baseline data on total organic carbon (TOC) concentrations in the coastal waters of the northern Persian Gulf. Limited published studies on TOC in the Gulf region are available^{29–31}. In this study, TOC concentrations ranged from 0.5 to 114.58 mg/L in winter and from 0.15 to 5.27 mg/L in summer. Figure 3 reveals that the highest concentration (114.58 ± 12.5 mg/L) was recorded at the Mond River station (M3) in winter, where the low salinity (1.8) suggests that riverine inputs and upstream rainfall significantly contributed to the elevated TOC levels (see Section “Measurement of physicochemical parameters”). A significant negative correlation ($r = -0.63$, $p < 0.05$) was observed between TOC and salinity in winter, suggesting that freshwater inputs may influence organic carbon levels. Previous studies, such as that by Al-Said et al., have found a strong inverse relationship between salinity and TOC near river mouths, including the Shatt Al-Arab³¹. Similar patterns of high TOC and dissolved organic carbon (DOC) concentrations have also been observed in other semi-enclosed seas, particularly in areas affected by river runoff^{32,33}.

The Secchi disc depth at station M3 was recorded at zero meters, indicating low water transparency, which is often associated with high concentrations of dissolved and colloidal inorganic and organic substances, suspended solids, and other materials that reduce water clarity (<http://helcom.fi/baltic-sea-trends/indicators/water-clarity>).

Changes in precipitation and river flow can influence the transport of DOC and TOC from terrestrial to aquatic systems, as highlighted by studies in the northeastern U.S. during extreme wet years³⁴. Similarly, Huntington et al., found that hydrological conditions can drive increased DOC export during winter months in rivers draining into the Gulf of Maine³⁵. Furthermore, the presence of iron and its complexes with DOC could also contribute to water clarity and high TOC levels, as documented by Weyhenmeyer et al.³⁶.

By excluding the TOC value at station M3 (an exceptionally high reading of 114.58 mg/L in winter), the overall average TOC concentration across both seasons is 3.24 ± 4.90 mg/L. This adjusted mean TOC value aligns with those previously reported from other marine systems, including the Persian Gulf. TOC concentrations in surface waters of the United Arab Emirates (UAE) and Qatar during 1986 ranged from 0.8 to 3.9 mg/L and from 0.5 to 3.6 mg/L, respectively³⁰. Emara noted higher TOC values in the UAE coastal areas, decreasing seaward³⁰. In the southern Persian Gulf and the Gulf of Oman, TOC concentrations ranged from 2.1 to 14.6 mg/L (mean 6.37 ± 3.7 mg/L) during February–March 1987, showing comparable values to this study²⁹. Surface TOC values in Kuwait and the northern Gulf from March 2014 to March 2016 ranged between 1.21 and 3.82 mg/L³¹. The highest TOC concentrations reported by Hansell and Peltzer in the northern Arabian Sea during the 1995 US JGOFS Arabian Sea Process Study were 0.96–1.2 mg/L in the surface layer³⁷. In the Indian, Pacific, and Atlantic Oceans, Starikova reported TOC levels ranging from 1.5 to 2.0 mg/L³⁸, while values in the Black Sea ranged from 2.5 to 3.0 mg/L. In the Northern Coastal Baltic Sea, TOC concentrations varied between 3 and 6 mg/L³⁹.

TPHs analysis

Figure 4 shows that the mean TPH concentrations in the surface waters of MPAs in winter and summer. The mean concentration levels of TPH ranged from ND to 134.63 mg/L in winter and ND to 20.26 mg/L in summer. Statistical analysis revealed a significant difference in mean TPH levels between the summer and winter seasons ($p < 0.05$). In summer, higher temperatures and increased evaporation rates lead to a decrease in petroleum hydrocarbons in the water. At station M1, the winter concentration of TPHs exceeded the recommended limit of 50 µg/L set by the Iran Department of Environment for seawater quality in the Persian Gulf and Gulf of Oman marine protected areas. This higher concentration may be attributed to river discharge into the estuary and shipping activities in the area. In other stations, TPH levels were below this permissible limit, indicating that TPH contamination is generally low in the studied area, except at station M1. The low TPH concentrations may also be due to sampling only surface waters and the high evaporation rates of these compounds.

For comparison (see Table 2), Akinola et al. reported TPH level ranging from not detected to 4.07 mg/L in coastal waters of Nigeria⁴⁰. Sayed et al. found TPH values ranging from 91 to 503 mg/L in coastal waters of Teluk Batik Beach, Malaysia⁴¹. Adeniji et al. reported TPH levels ranging from 0.045 to 0.273 mg/L in the surface

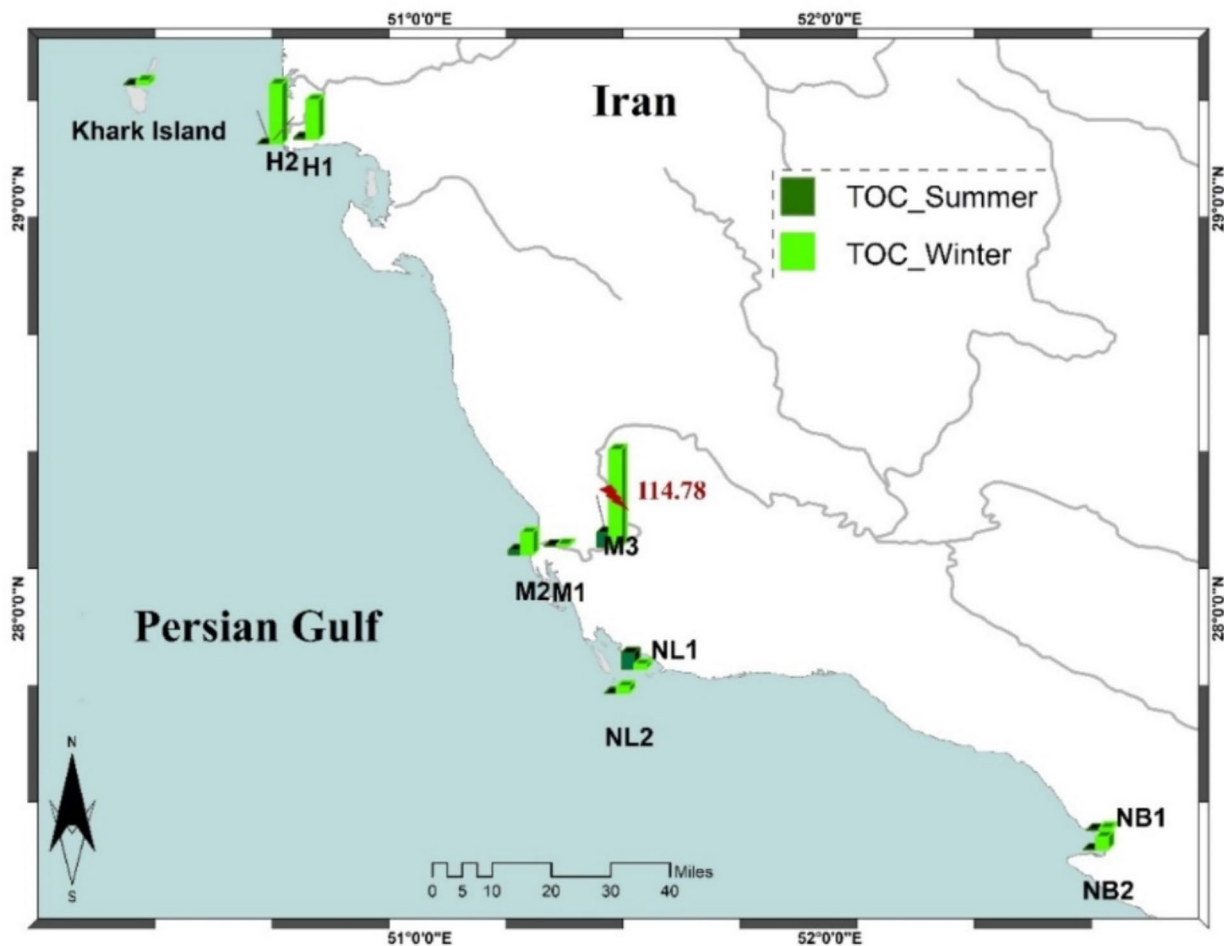


Fig. 3. The mean concentrations of TOC (mg/L) in the surface waters of MPAs in winter and summer. The map was created using Esri ArcMap, version 10.3 (available at <https://desktop.arcgis.com/en/arcmap/10.0/>).

waters of Algoa Bay, Eastern Cape, South Africa⁴². In Tianjin Bohai Bay, the TPH concentration varied widely from 0.020 to 0.508 mg/L between 1996 and 2005⁴³.

Anionic surfactants analysis

Surfactants are organic compounds present in the ocean from both anthropogenic and natural sources that can influence biogeochemical cycles⁶². Accumulation of surfactants in the surface microlayer can negatively impact marine and freshwater organisms⁶².

In this study, the mean concentrations of anionic surfactants ranged from 10 to 79 $\mu\text{g/L}$ in winter and 11 to 30 $\mu\text{g/L}$ in summer. Seasonal comparisons (see Fig. 5) revealed that anionic surfactant levels were higher in winter than in summer, with the highest concentration of 79 $\mu\text{g/L}$ observed at the Mond River mouth (M1). Seasonal variations in temperature and light affect chemical reaction rate, which in turn influence the degradation, persistence, and mobility of pollutants in the marine environment. Higher temperatures and increased light in summer typically accelerate the breakdown of certain contaminants, while lower temperatures in winter may slow down these processes⁶³. Sales et al. noted that higher temperatures and light levels accelerate the biodegradation of anionic surfactants⁶³. Therefore, the higher surfactant concentrations in winter could be attributed to lower surface water temperatures and reduced biodegradation. Takada et al. observed that anionic surfactant concentrations in winter were about ten times higher than in summer for the same reason⁶⁴. Additionally, seasonal rainfall variations influence river discharge and flow rates, which can transport more surfactants to the M1 station. This increase might also be linked to agricultural and mariculture activities upstream of the Mond River.

Shaharom et al. reported that surfactant concentrations in the surface microlayer at various coastal stations in Peninsular Malaysia ranged from 0.23 to 0.35 $\mu\text{mol/L}$, while subsurface water concentrations ranged from 0.20 to 0.32 $\mu\text{mol/L}$ ⁶⁵. To expand on these findings, future research should include the determination of biomarkers or organic tracers to identify primary sources of surfactants in seawater. Additionally, analyzing nutrient concentrations (e.g., phosphates and nitrogen) could provide a better understanding of surfactant levels in seawater.

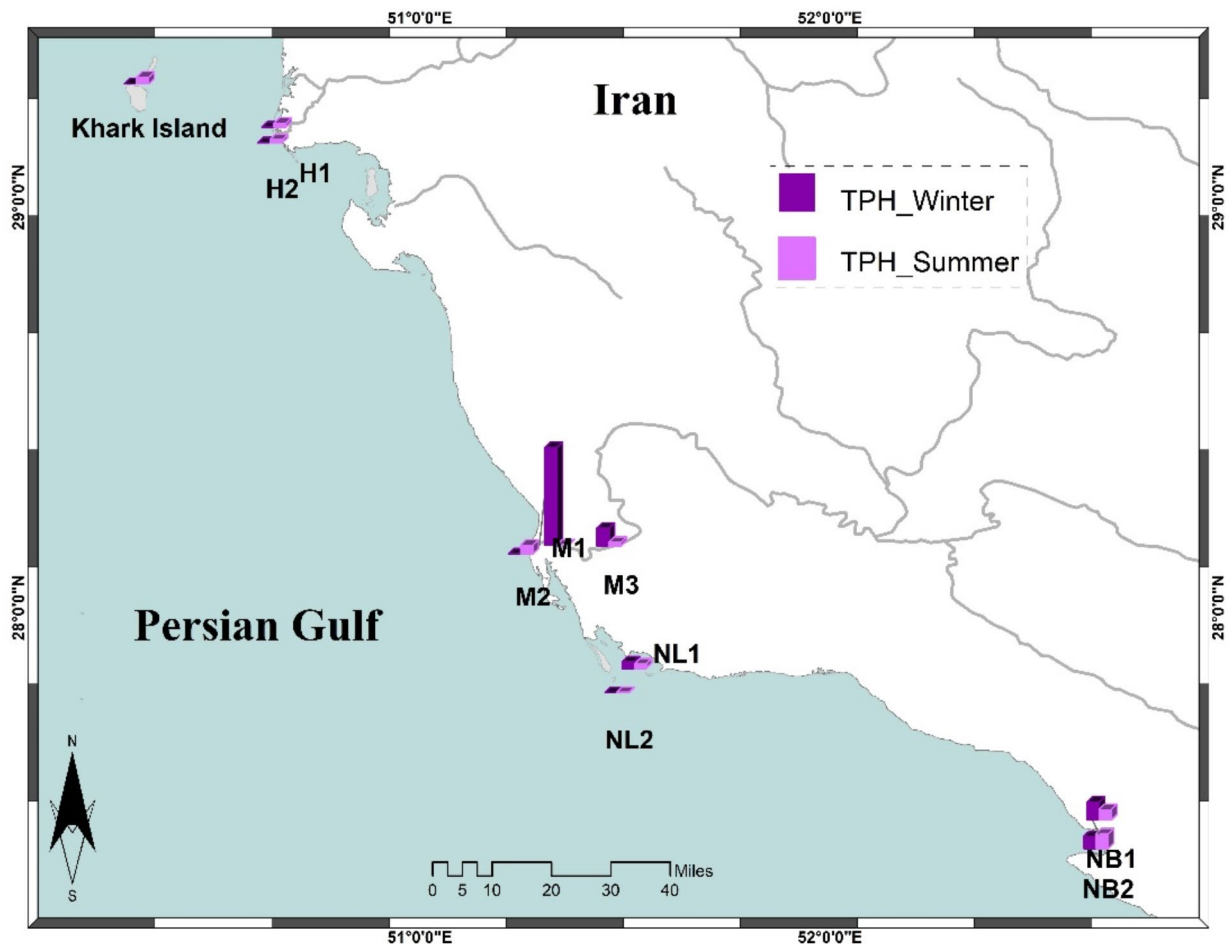


Fig. 4. The mean concentrations of TPH (mg/L) in the surface waters of MPAs in winter and summer. The map was created using Esri ArcMap, version 10.3 (available at <https://desktop.arcgis.com/en/arcmap/10.0/>).

According to the World Health Organization (WHO), the permissible limit for anionic surfactants in surface water is 1 mg/L, while the Bureau of Indian Standards (BIS) sets a permissible limit of 0.2 mg/L for surface water⁶⁶. In Japan, the Ministry of Health, Labor, and Welfare has established permissible levels for anionic surfactants in drinking water at 0.2 mg/L⁶⁷. Several environmental and public health authorities have implemented strict standards, such as 0.5 mg/L for anionic detergents in drinking water and up to 1 mg/L for other uses⁶⁸. Italian legislation allows concentrations of 0.2 mg/L for drinking water, 2 mg/L for surface water, 4 mg/L for sewage, and 0.5 mg/L for agricultural reuse^{67,69}. The concentration range of anionic surfactants in this study were lower than the global permissible values.

OCPs analysis

Organochlorine pesticides (OCPs) are persistent, anthropogenic chemicals with the potential for bioaccumulation, long-range atmospheric transport, and toxicity to both wildlife and humans^{70,71}. Among OCPs, isomeric forms of hexachlorocyclohexane (HCHs) and dichlorodiphenyltrichloroethanes (DDTs) are frequently studied in marine environmental pollution research. Aside from HCHs and DDTs, there is limited data on other OCPs in seawater. This study represents the first measurement of 17 OCPs, including HCHs (α -HCH, β -HCH, γ -HCH, and δ -HCH), DDTs (*p*, *p'*-DDE, *p*, *p'*-DDD, and *p*, *p'*-DDT), Heptachlor, Aldrin, Alpha-Heptachlorepoxyde, Endosulfan II, Dieldrin, Endrin, Endosulfan I, Endrin-aldehyde, Endosulfan-sulfate, and Methoxychlor in the marine protected areas of the Persian Gulf.

Figure 6 shows that the mean OCP concentrations in the surface waters of MPAs varied spatially and seasonally. The total concentrations of 17 OCPs were 3.13–112.98, and 58.54–219.6 ng/L in winter and summer, respectively. In summer, HCHs were present at all stations, with the highest concentration of 141.28 ng/L recorded at station M1. In winter, the highest value of HCHs were detected at M1 with a concentration of 96.26 ng/L, suggesting a likely local origin. The presence of agricultural and mariculture activities upstream could contribute to this increase. The sources and residue levels of OCPs in water are influenced by the extent of agricultural pesticide use in the catchment area⁵⁴. In winter, OCPs showed a significant positive correlation with TPHs ($r=0.98$, $p<0.01$), PCBs ($r=0.81$, $p<0.01$), and anionic surfactant ($r=0.64$, $p<0.05$). In summer, the

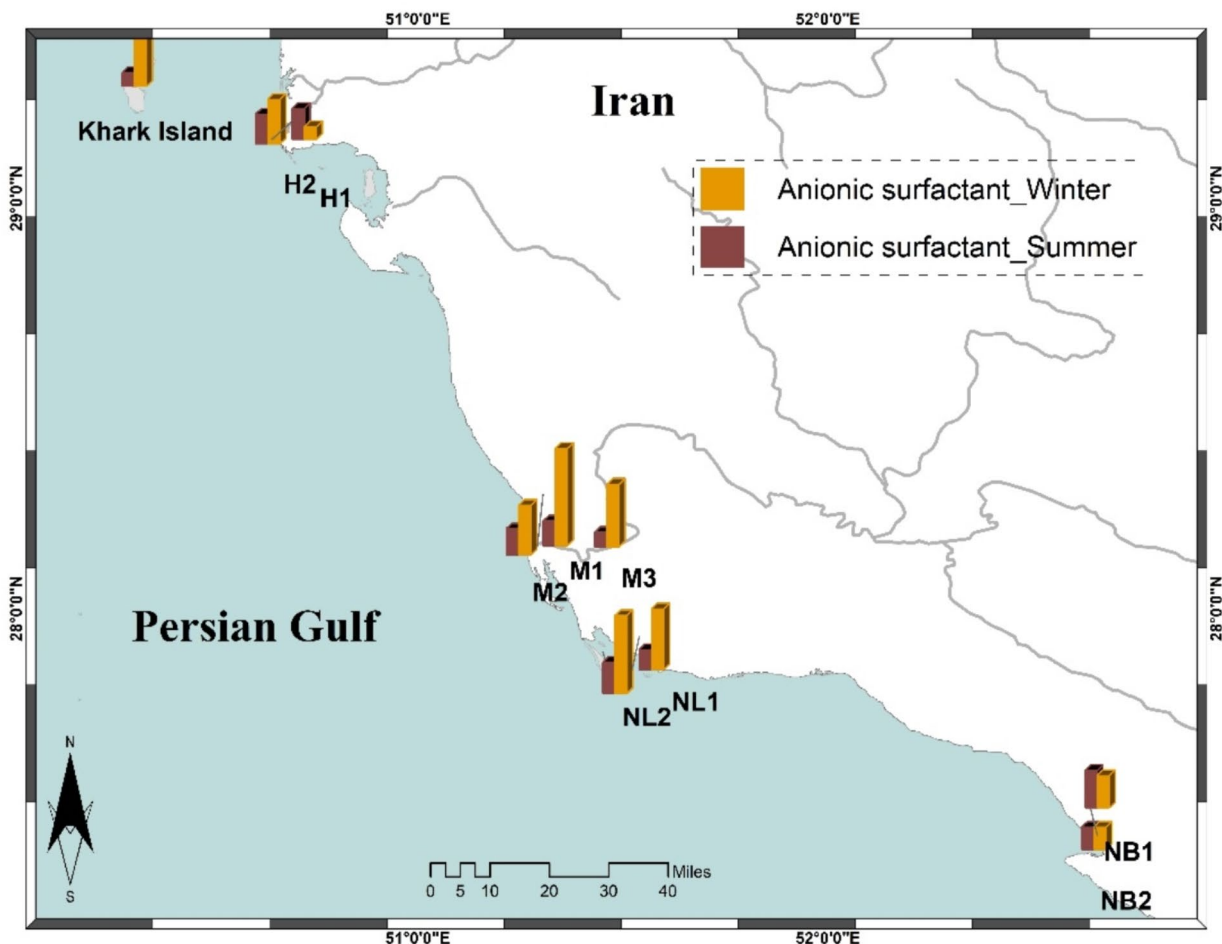


Fig. 5. The mean concentrations ($\mu\text{g/L}$) of anionic surfactants in the surface waters of MPAs in winter and summer. The map was created using Esri ArcMap, version 10.3 (available at <https://desktop.arcgis.com/en/arcmap/10.0/>).

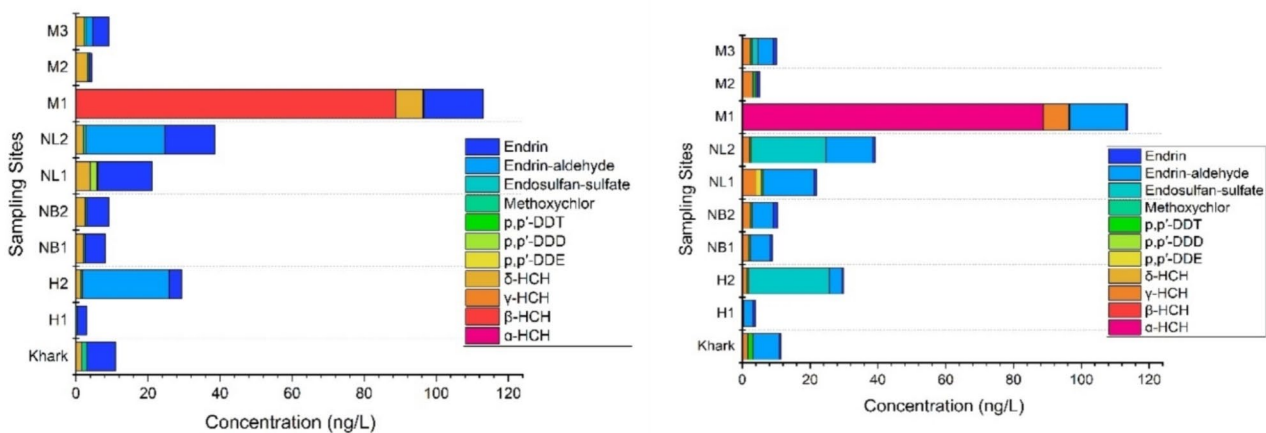


Fig. 6. The mean OCP concentrations in the surface waters of MPAs in winter (right) and summer (left).

OCPs showed significant positive correlation ($r=0.81$, $p<0.01$) with TPHs. This may imply that these pollutants have a common origin (potential local usage and residue release).

Internationally, the average concentration of total HCHs is reported as 0.41 ng/L in the Bering Sea and 0.44 ng/L in the Chukchi Sea⁵². In contrast, HCH concentrations in Bohai Bay and Daya Bay ranged from 50 to 750 ng/L (mean 160 ng/L)⁵³ and 36 to 1229 ng/L (mean 285 ng/L)⁴⁶, respectively. Seawater in Singapore, the southern Baltic Sea, and offshore Mumbai (India) had HCH concentrations below 100 ng/L. Areas such as Haimen Bay, Xinghua Bay, Deep Bay, northern South China Sea, and coastal Hong Kong exhibited low HCH levels (<20 ng/L)⁵⁴. HCB concentrations in the Northern South China Sea (NSCS) and East China Sea (ECS) were significantly higher in summer compared to other seasons, with average values of 0.59 ± 0.55 ng/L in spring and 2.5 ± 2.0 ng/L in summer for NSCS, and 0.13 ± 0.19 ng/L in spring and 1.4 ± 0.48 ng/L in summer for ECS⁴⁷. Han and Currel, reported HCH concentrations in China's seawaters ranging from $<LOD$ to 1228.6 ng/L (mean 0.6 to 285 ng/L), which are considerably lower than the Chinese seawater quality standard (GB3097-1997) of <1000 ng/L⁵⁴. The concentrations of HCHs in the present study were much lower than this standard.

In summer, DDTs were not detected in the study stations and were only present in station M3 in winter (1.71 ng/L). This station is located in the Mond River, and the reason could be associated with land-source inputs by surface runoff and the transfer from the upstream catchment (see Section "Measurement of physicochemical parameters").

Said et al., measured concentrations of organochlorine contaminants including DDTs, PCBs, and HCHs in water, sediments and biota of the lake Burullus, along the Egyptian Mediterranean Sea coast⁴⁴. The concentrations of DDTs in water were ranged from 0.07 to 221.9 ng/L; 46.3–656.5 ng/L; 94.3–882.6 ng/L, and 24.8–233 ng/L during winter, spring, summer and autumn, respectively⁴⁴. The average concentrations of DDTs were ranged from 0.22 to 16.86 ng/L in surface water of Alexandria, Egypt⁴⁵. The average HCHs concentration in near-shore surface water of Alexandria was 0.16–0.63⁴⁵.

The Chinese seawater quality standard for DDTs is <50 ng/L, and concentrations in Chinese seawaters range from $<LOD$ to 975.9 ng/L (mean 0.5–175.0 ng/L)⁵⁴. Significant DDT contamination was reported in Daya Bay (27–975 ng/L, mean 175 ng/L)⁴⁶. DDT contamination was also detected in seawater samples collected from Bohai Bay, Macao Harbor, Sanggou Bay, South China Sea, and Xinghua Bay, with values at the upper range beyond 50 ng/L⁵⁴. Seawater samples from Deep Bay, Hong Kong, Laizhou Bay, Haimen Bay, and Xiamen Harbor showed lower DDT contamination (<25 ng/L). The mean ΣDDT in Laguna de Terminos, Mexico, was 0.28 ng/L (range 0.07–0.60 ng/L)⁵⁵. The mean ΣDDT in the NSCS in spring, summer, autumn, and winter were 0.22 ± 0.19 , 2.2 ± 2.0 , 1.3 ± 1.4 , and 0.16 ± 0.46 ng/L, respectively. They were 0.23 ± 0.12 , 1.6 ± 1.3 , 0.53 ± 0.27 , and 0.54 ± 0.25 ng/L, in the ECS, in the corresponding seasons⁴⁷.

Throughout both seasons, endosulfan-sulfate was below the limit of detection at all stations except M3 in summer (0.67 ng/L). Endrin was detected at all stations, with the highest concentrations being 33.11 ng/L in summer (station NB2) and 16.40 ng/L in winter (M1 station). Aldrin, alpha-heptachlorepoxyde, heptachlor, endosulfan I, endosulfan II, and dieldrin were not detected in either season, and therefore are not shown in Fig. 6.

The concentrations of endrin were ranged from 0.67 to 87.58 ng/L; nd-124.74 ng/L; 3.81–108.70 ng/L, and 0.96–68.90 ng/L during winter, spring, summer, and autumn, respectively in Lake Burullus⁴⁴. The average endrin concentration in near-shore surface water of Alexandria, Egypt was 0.001–0.015 ng/L⁴⁵.

In the Bering Sea, mean concentrations of endrin, dieldrin, and endosulfan I was 0.052, 0.033, and 0.101 ng/L, respectively⁵². Aldrin and endosulfan II were below detection limits in the Bering Sea, but had mean values of 0.077 and 0.035 ng/L, respectively, in the Chukchi Sea⁵². Endosulfan sulfate and endrin aldehyde were not detected in either study area. In surface water of the Laguna de Terminos, a protected area of the coast of Campeche, Mexico, lindane (mean 0.021 ng/L), endosulfan (mean 0.015 ng/L), and chlordane (mean 0.018 ng/L) were measured⁵⁸. In three main estuaries at Cirebon coastal water, West Java Province, Indonesia, OCP concentrations in seawater ranged from 10 to 120 ng/L (mean 32 ± 36 ng/L), with dieldrin being the dominant pollutant⁷².

The European Union (EU) Directive sets the Maximum Contaminant Level (MCL) for each individual OCP in surface water at 0.1 $\mu\text{g/L}$, and the total concentration for all OCPs at 0.5 $\mu\text{g/L}$. According to the EU Water Framework Directive (EU WFD), aldrin, dieldrin, and endrin levels in marine waters should remain below 5 ng/L. According to Tornero et al., the total concentration of DDT should not exceed 25 ng/L, DEHP should be limited to 1300 ng/L, endosulfan to 0.5 ng/L, and heptachlor to 0.00001 ng/L⁷³.

According to Iran's Department of Environment standards for seawater quality in the Persian Gulf and Gulf of Oman MPAs, the sum of DDT, DDE, DDD, lindane, α -HCH, and β -HCH should be <10 ng/L. In summer, concentrations of these six OCPs exceeded the permissible limit at all stations, with the highest value at M1. In winter, the total concentration was below the permissible limit, except at station M1.

Overall, higher OCP concentrations were observed in surface waters near agricultural and maricultural areas in the Mond River and estuary, suggesting that these activities are significant sources of OCPs in this region. Agriculture and mariculture are crucial economic activities in this area, and Iran, accounting for 0.2% of global pesticide use, continues to utilize OCPs despite ratifying the Stockholm Convention in May 2005. The use of these pesticides has been linked to contamination in pregnant women's hair and breast milk^{74,75} and in agricultural soils in southern Iran⁷⁶. The lack of proper training for farmers and awareness of environmental threats contributes to the uncontrolled use of these pollutants⁷⁷. Despite ratification of the Stockholm Convention, soil contamination with OCPs in southern Iran remains a concern.

PCBs analysis

Figure 7 shows the mean concentrations of 19 PCBs, including PCB-28, PCB-52, PCB-101, PCB-81, PCB-77, PCB-123, PCB-118, PCB-114, PCB-153, PCB-105, PCB-138, PCB-126, PCB-167, PCB-156, PCB-157, PCB-180,

PCB-169, PCB-189, in the surface water of the MPAs in winter and summer. PCB concentrations in seawater exhibited significant spatial and seasonal variation (one-way ANOVA and one-sample t-test, $p < 0.05$). The mean concentration of $\Sigma 19$ PCBs (ng/L) ranged from 0.72 at station M2 to 4.66 at station M1 during winter, and from 2.49 at Khark Coral Island to 5.05 at NL1 station during summer. Statistical analysis revealed that PCB levels in summer and winter were significantly different at all stations except MPA24 ($p < 0.05$).

As shown in Table 2, the range of PCB concentrations found in this study was substantially lower than those reported in many coastal waters, such in Shadegan Wetland, northwestern Persian Gulf⁵⁷; Lake Burullus, Egypt⁴⁴; Bay of Bengal coast of Bangladesh⁵⁹; and Alexandria coasts, Egypt⁴⁵. However, the levels found here were higher than those in Laguna de Terminos, a protected area off the coast of Campeche, Mexico (0.07–3.40 ng/L, mean 1.18 ng/L)⁵⁵, but similar to those at Larak Coral Island in the Persian Gulf, Iran (0.97–3.10 ng/L)⁵⁸.

Regarding toxicity and bioaccumulation properties of PCBs as carcinogenic and persistent organic pollutants^{76,77}, besides the ecological importance of the coastal area of the Persian Gulf, it is necessary to assess the potential environmental risk of PCBs in this region.

When compared to national and international standards, the concentrations of Σ PCBs in surface water (0.72–4.66 ng/L in winter and 2.79–5.05 ng/L in summer) are below the criterion maximum concentration (CMC) set by the US National Oceanic and Atmospheric Administration (NOAA) for water quality, which is 10,000 ng/L for coastal water and 20 ng/L for inland water.

According to Iran's Department of Environment standards, Σ PCBs concentrations in all studied areas and seasons were below the permissible limits for the Persian Gulf and Gulf of Oman marine protected areas (10 ng/L). These concentrations were also lower than the standard continuous concentration (30 ng/L for coastal water and 14 ng/L for inland water) recommended by the US EPA and NOAA to protect aquatic and human health from chronic exposure to dissolved PCBs⁷⁸. Additionally, the Σ PCBs levels were below the Chinese national environmental quality standard for Σ PCBs in surface water (20 ng/L). Thus, the surface waters of the MPAs in Bushehr province, Iran, are currently not polluted with PCBs. Continued efforts and control actions are highly recommended to maintain these conditions. Our data can serve as a baseline for management planning and future research on these compounds in the Persian Gulf.

Conclusion

This study provides the first comprehensive investigation of persistent organic pollutants (POPs), including OCPs, PCBs, TPHs, and anionic surfactants, in the seawaters of Marine Protected Areas in the northern Persian Gulf. The findings reveal significant seasonal and spatial variations in pollutant concentrations, with the Mond protected area identified as a major pollution hotspot. Elevated levels of TPHs and OCPs, particularly in the winter, point to pollution from agricultural and maricultural runoff, industrial activities, and riverine inputs.

Although PCBs were below permissible limits, the high levels of TPHs and OCPs in certain areas exceed both national and international standards, raising concerns about the effectiveness of current conservation efforts in these MPAs. The results suggest that MPA designation alone may not provide adequate protection from pollution, highlighting the need for more stringent management and pollution control measures.

Given the pollution pressures faced by the region, there is an urgent need to prioritize monitoring, regulation, and conservation efforts in the Mond protected area and other vulnerable zones. Continued research and long-term monitoring are essential to safeguard these critical marine ecosystems from further degradation.

Data availability

The datasets used and/or analysed during the current study available from the corresponding author on reasonable request.

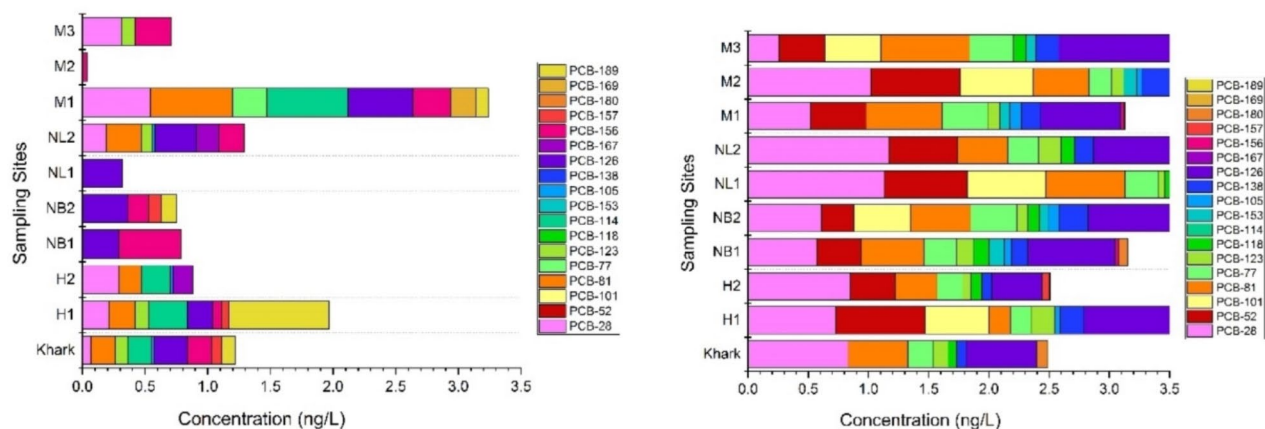


Fig. 7. The mean PCBs concentrations in the surface waters of MPAs in winter (right) and summer (left).

References

- Breida, M., Younssi, S. A., Ouammou, M., Bouhria, M. & Hafsi, M. Pollution of water sources from agricultural and industrial effluents: special attention to 3^+ , Cr (vi), and Cu (ii). *Water Chem.* **39** (2019).
- Haghshenas, A., Hatami-manesh, M., Mirzaei, M., Mir Sanjari, M. & Khezri, H. Measurement and evaluation of ecological risk of heavy metals in surface sediments of pars Special Economic Energy Zone. *ISMJ.* **20**, 448–469 (2017).
- Mateo-Sagasta, J., Zadeh, S. M., Turrall, H. & Burke, J. Water pollution from agriculture: A global review. *Exec. Summary* (2017).
- Tornero, V. & Hanke, G. Chemical contaminants entering the marine environment from sea-based sources: a review with a focus on European seas. *Mar. Pollut. Bull.* **112**, 17–38 (2016).
- Wasewar, K. L., Singh, S. & Kansal, S. K. Process intensification of treatment of inorganic water pollutants. In *Inorganic Pollutants in Water* 245–271 (Elsevier, 2020).
- Reid, W. V. et al. In *Ecosystems and Human Well-Being-Synthesis: A Report of the Millennium Ecosystem Assessment* (Island, 2005).
- OECD. *Marine Protected Areas: Economics, Management and Effective Policy Mixes* (OECD Publishing Paris, 2017).
- Bijma, J., Pörtner, H. O., Yesson, C. & Rogers, A. D. Climate change and the oceans: What does the future hold? *Mar. Pollut. Bull.* **74**, 495–505 (2013).
- Clarke Murray, C., Mach, M. E. & Martone, R. G. *Cumulative Effects in Marine Ecosystems: Scientific Perspectives on Its Challenges and Solutions* (World Wildlife Fund Canada, 2014).
- Korpinen, S. et al. Multiple pressures and their combined effects in Europe's seas (2020).
- Massoud, M. S., Al-Abdali, F., Al-Ghadban, A. N. & Al-Sarawi, M. Bottom sediments of the Arabian Gulf—II. TPH and TOC contents as indicators of oil pollution and implications for the effect and fate of the Kuwait oil slick. *Environ. Pollut.* **93**, 271–284 (1996).
- Price, A. The Gulf: Human impacts and management initiatives. *Mar. Pollut. Bull.* **27**, 17–27 (1993).
- Sheppard, C. R. Physical environment of the Gulf relevant to marine pollution: An overview. *Mar. Pollut. Bull.* **27**, 3–8 (1993).
- Vaezi, A. & Lak, R. Contamination and environmental risk assessment of potentially toxic elements in the surface sediments of Northwest Persian Gulf. *Reg. Stud. Mar. Sci.* **67**, 103235 (2023).
- Reynolds, R. M. Physical oceanography of the Gulf, Strait of Hormuz, and the Gulf of Oman—Results from the Mt Mitchell expedition. *Mar. Pollut. Bull.* **27**, 35–59 (1993).
- Kor, K. & Mehdiinia, A. Neustonic microplastic pollution in the Persian Gulf. *Mar. Pollut. Bull.* **150**, 110665 (2020).
- Fowler, S. W., Readman, J. W., Oregioni, B. J. P. V., Villeneuve, J. P. & McKay, K. Petroleum hydrocarbons and trace metals in nearshore Gulf sediments and biota before and after the 1991 war: An assessment of temporal and spatial trends. *Mar. Pollut. Bull.* **27**, 171–182 (1993).
- Kelleher, G. Guidelines for marine protected areas: IUCN, Gland, Switzerland and Cambridge, UK (1999).
- Selig, E. R. et al. Global priorities for marine biodiversity conservation. *PLoS ONE.* **9**, e82898 (2014).
- Edgar, G. J. et al. Global conservation outcomes depend on marine protected areas with five key features. *Nature.* **506**, 216–220 (2014).
- Halpern, B. S. et al. A global map of human impact on marine ecosystems. *Science.* **319**, 948–952 (2008).
- Abessa, D. M. et al. Pollution status of marine protected areas worldwide and the consequent toxic effects are unknown. *Environ. Pollut.* **243**, 1450–1459 (2018).
- Jameson, S. C., Tupper, M. H. & Ridley, J. M. The three screen doors: Can marine protected areas be effective? *Mar. Pollut. Bull.* **44**, 1177–1183 (2002).
- Pouladi, M., Qadermarzi, A., Baharvand, F., Vazirizadeh, A. & Hedayat, A. Effects of physicochemical factors on seasonal variations of phytoplankton in the Mond River Estuary of Bushehr Province, Persian Gulf, Iran. *Biodivers. J. Biolog Divers.* **18** (2017).
- Hosseini, S. T. & Siadatmousavi, S. M. Field observations of hypersaline runoff through a shallow estuary. *Estuar. Coast Shelf Sci.* **202**, 54–68 (2018).
- Ghaemi, M. & Gholamipour, S. Seasonal measurement of nutrient concentrations and total alkalinity in the Mond Estuary ecosystem. *J. Oceanogr.* **8**, 11–18 (2017).
- Environmental, F. Conductivity, salinity and total dissolved solids: fundamentals of environmental measurements (2014).
- O'Boyle, S., McDermott, G. & Wilkes, R. Dissolved oxygen levels in estuarine and coastal waters around Ireland. *Mar. Pollut. Bull.* **58**, 1657–1663 (2009).
- Emara, H. I. Nutrient salts, inorganic and organic carbon contents in the waters of the Persian Gulf and the Gulf of Oman. *J. Persian Gulf.* **1**, 33–44 (2010).
- Emara, H. I. Total organic carbon content in the waters of the Arabian Gulf. *Environ. Int.* **24**, 97–103 (1998).
- Al-Said, T., Naqvi, S. W. A., Al-Yamani, F., Goncharov, A. & Fernandes, L. High total organic carbon in surface waters of the northern Arabian Gulf: Implications for the oxygen minimum zone of the Arabian Sea. *Mar. Pollut. Bull.* **129**, 35–42 (2018).
- Sempere, R., Panagiotopoulos, C., Lafont, R., Marroni, B. & Van Wambeke, F. Total organic carbon dynamics in the Aegean Sea. *J. Mar. Syst.* **33**, 355–364 (2002).
- Wang, X. C., Chen, R. F. & Gardner, G. B. Sources and transport of dissolved and particulate organic carbon in the Mississippi River estuary and adjacent coastal waters of the northern Gulf of Mexico. *Mar. Chem.* **89**, 241–256 (2004).
- Strock, K. E. et al. Extreme weather years drive episodic changes in lake chemistry: Implications for recovery from sulfate deposition and long-term trends in dissolved organic carbon. *Biogeochem.* **127**, 353–365 (2016).
- Huntington, T. G. et al. Climate change and dissolved organic carbon export to the Gulf of Maine. *J. Geophys. Res. Biogeosci.* **121**, 2700–2716 (2016).
- Weyhenmeyer, G. A., Prairie, Y. T. & Tranvik, L. J. Browning of boreal freshwaters coupled to carbon-iron interactions along the aquatic continuum. *PLoS ONE.* **9**, e88104 (2014).
- Hansell, D. A. & Peltzer, E. T. Spatial and temporal variations of total organic carbon in the Arabian Sea. *Deep-Sea Res. II Top. Stud. Oceanogr.* **45**, 2171–2193 (1998).
- Starikova, N. D. Vertical distribution patterns of dissolved organic carbon in sea water and interstitial solutions. *Oceanology (Ussr).* **10**, 796–807 (1970).
- Fleming-Lehtinen, V., Råike, A., Kortelainen, P., Kauppila, P. & Thomas, D. N. Organic carbon concentration in the northern coastal Baltic Sea between 1975 and 2011. *Estuar. Coasts.* **38**, 466–481 (2015).
- Akinola, J. O., Olawusi-Peters, O. O. & Akpambang, V. O. E. Ecological hazards of total petroleum hydrocarbon in brackish water white shrimp *Nematopalaemon hastatus* (AURIVILLUS 1898). *Egypt. J. Aquat. Res.* **45**, 205–210 (2019).
- Sayed, K., Baloo, L., Yekken, S. T., Kankia, M. U. & Jagaba, A. H. Determination of total petroleum hydrocarbons concentration in coastal seawater of Teluk Batik Beach, Perak, Malaysia. *Key Eng. Mater.* **888**, 119–128 (2021).
- Adeniji, A. O., Okoh, O. O. & Okoh, A. I. Petroleum hydrocarbon profiles of water and sediment of Algoa Bay, Eastern Cape, South Africa. *Int. J. Environ. Res. Public Health.* **14**, 1263 (2017).
- Li, Y., Zhao, Y., Peng, S., Zhou, Q. & Ma, L. Q. Temporal and spatial trends of total petroleum hydrocarbons in the seawater of Bohai Bay, China from 1996 to 2005. *Mar. Pollut. Bull.* **60**, 238–243 (2010).

44. Said, T. O., Moselhy, E., Rashad, K. M., Shreadah, M. A. & A. A. M., & Organochlorine contaminants in water, sediment and fish of Lake Burullus, Egyptian Mediterranean Sea. *Bull. Environ. Contam. Toxicol.* **81**, 136–146 (2008).
45. Said, T. O., Okbah, M. A., Mohamed, L. A. & Othman, I. M. Detection of persistent OCPs and PCBs congeners in the near-shore coastal waters of Alexandria, Egypt. *Environ. Monit. Assess.* **187**, 1–13 (2015).
46. Qiu, Y. et al. Study on polychlorinated biphenyl congeners and organochlorine insecticides in Daya Bay. *Mar. Environ. Sci. / Haiyang Huanjing Kexue.* **21**, 46–51 (2002).
47. Ya, M. et al. Impacts of seasonal variation on organochlorine pesticides in the East China Sea and Northern South China Sea. *Environ. Sci. Technol.* **53**, 13088–13097 (2019).
48. Zhang, L. et al. Contamination characteristics, spatial distribution and ecological-health risk assessment of legacy and current-use pesticides: A case study in the Beibu Gulf. *Front. Mar. Sci.* **10**, 1167712 (2023).
49. Lammel, G. et al. Organochlorine pesticides and polychlorinated biphenyls along an east-to-west gradient in subtropical North Atlantic surface water. *Environ. Sci. Pollut. Res.* **24**, 11045–11052 (2017).
50. Zhang, Z. L., Hong, H. S., Zhou, J. L., Huang, J. & Yu, G. Fate and assessment of persistent organic pollutants in water and sediment from Minjiang River Estuary, Southeast China. *Chemosphere.* **52**, 1423–1430 (2003).
51. Lin, T. et al. Organochlorine pesticides in seawater and the surrounding atmosphere of the marginal seas of China: Spatial distribution, sources and air–water exchange. *Sci. Tot Environ.* **435**, 244–252 (2012).
52. Yao ZiWei, Y. Z., Jiang GuiBin, J. G. & Xu HengZhen, X. H. Distribution of organochlorine pesticides in seawater of the Bering and Chukchi Sea. *Environ. Pollut.* **116**, 49–56 (2002).
53. Wang, T. et al. Occurrence of dissolved polychlorinated biphenyls and organic chlorinated pesticides in the surface water of Haihe River and Bohai Bay, China. *Huan Jing Ke Xue = Huanjing Kexue.* **28**, 730–735 (2007).
54. Han, D. & Currell, M. J. Persistent organic pollutants in China's surface water systems. *Sci. Tot Environ.* **580**, 602–625 (2017).
55. Carvalho, F. P., Villeneuve, J. P., Cattini, C., Rendón, J. & de Oliveira, J. M. Pesticide and PCB residues in the aquatic ecosystems of Laguna De Terminos, a protected area of the coast of Campeche, Mexico. *Chemosphere.* **74**, 988–995 (2009).
56. D'Agostino, F. et al. Persistent and emerging organic pollutants in the marine coastal environment of the Gulf of Milazzo (Southern Italy): Human health risk assessment. *Front. Environ. sci.* **8**, 117 (2020).
57. Zahed, M. A., Bidhendi, N., Pardakhti, G., Esmaili-Sari, A., Mohajeri, S. & A., & Determination of polychlorinated biphenyl congeners in water and sediment in North West Persian Gulf, Iran. *Bull. Environ. Contam. Toxicol.* **83**, 899–902 (2009).
58. Jafarabadi, A. R. et al. First polychlorinated biphenyls (PCBs) monitoring in seawater, surface sediments and marine fish communities of the Persian Gulf: Distribution, levels, congener profile and health risk assessment. *Environ. Pollut.* **253**, 78–88 (2019).
59. Habibullah-Al-Mamun, M., Ahmed, M. K., Islam, M. S., Tokumura, M. & Masunaga, S. Occurrence, distribution and possible sources of polychlorinated biphenyls (PCBs) in the surface water from the Bay of Bengal coast of Bangladesh. *Ecotoxicol. Environ. Saf.* **167**, 450–458 (2019).
60. Sur, M. Distributions of anionic surfactant in sea water and total organic carbon in bottom-surface sediment along the Turkish coast of the Black Sea. *Turk. J. Fish. Aquat. Sci.* **15**, 677–690 (2015).
61. Pastewski, S. & Medrzycka, K. Monitoring surfactant concentrations in surface waters in tricity agglomeration. *Pol. J. Environ. Stud.* **12**, 643–646 (2003).
62. Olkowska, E., Ruman, M., Kowalska, A. & Polkowska, Ż. Determination of surfactants in environmental samples. Part II. Anionic compounds. *Ecol. Chem. Eng. S.* **20**, 331–342 (2013).
63. Sales, D., Perales, J. A., Manzano, M. A. & Quiroga, J. M. Anionic surfactant biodegradation in seawater. *Bol. Inst. Esp. Oceanogr.* **15**, 517–522 (1999).
64. Takada, H., Ogura, N. & Ishiwatari, R. Seasonal variations and modes of riverine input of organic pollutants to the coastal zone: 1. Flux of detergent-derived pollutants to Tokyo Bay. *Environ. sci. Technol.* **26**, 2517–2523 (1992).
65. Shaharom, S. et al. Surfactants in the sea surface microlayer, subsurface water and fine marine aerosols in different background coastal areas. *Environ. Sci. Pollut. Res.* **25**, 27074–27089 (2018).
66. Bureau of Indian Standards (BIS). Specification for drinking water 1S:10500: Bureau of Indian Standards, New Delhi (1991).
67. Borghi, C. C., Fabbri, M., Fiorini, M., Mancini, M. & Ribani, P. L. Magnetic removal of surfactants from wastewater using micrometric iron oxide powders. *Sep. Purif. Technol.* **83**, 180–188 (2011).
68. Rao, A. R., Pusey, D. I., Cooper, T. & Hamed, K. H. Monitoring wastewater flows on a university campus. In *Water Resources Engineering 1744–1748* (ASCE, 1995).
69. Ferella, F., De Michelis, I., Zerbini, C. & Vegliò, F. Advanced treatment of industrial wastewater by membrane filtration and ozonization. *Desalination.* **313**, 1–11 (2013).
70. Stemmler, I. & Lammel, G. Cycling of DDT in the global environment 1950–2002: World ocean returns the pollutant. *Geophys. Res. Lett.* **36** (2009).
71. Willett, K. L., Ulrich, E. M. & Hites, R. A. Differential toxicity and environmental fates of hexachlorocyclohexane isomers. *Environ. Sci. Technol.* **32**, 2197–2207 (1998).
72. Yogaswara, D., Wulandari, I., Hindarti, D. & Falahudin, D. Organochlorine pesticides in marine sediments and seawater from Cirebon coastal water, West Java, Indonesia: Concentration, spatial distribution, potential sources, and ecological risk assessment. *Mar. Pollut. Bull.* **180**, 113758 (2022).
73. Tornero, V. et al. Development and Implementation of Marine Contaminant Threshold Values (2022).
74. Behrooz, R. D., Barghi, M., Bahramifar, N. & Esmaili-Sari, A. Organochlorine contaminants in the hair of Iranian pregnant women. *Chemosphere.* **86**, 235–241 (2012).
75. Behrooz, R. D., Sari, A. E., Bahramifar, N. & Ghasempouri, S. M. Organochlorine pesticide and polychlorinated biphenyl residues in human milk from the Southern Coast of Caspian Sea, Iran. *Chemosphere.* **74**, 931–937 (2009).
76. Kafaei, R. et al. Organochlorine pesticides contamination in agricultural soils of southern Iran. *Chemosphere.* **240**, 124983 (2020).
77. Sharafi, K. et al. Knowledge, attitude and practices of farmers about pesticide use, risks, and wastes; a cross-sectional study (Kermanshah, Iran). *Sci. Tot Environ.* **645**, 509–517 (2018).
78. EPA U. *National Recommended Water Quality Criteria*. United States Environmental Protection Agency' (Office of Water, Office of Science and Technology, 2009).

Acknowledgements

This work was carried out with joint research funding from the Iranian National Institute for Oceanography and Atmospheric Science (INIOAS) and the Iran National Environment Fund (INEF) under project no. 9310/1020571.

Author contributions

All authors have agreed to be listed and have approved the submitted version of the manuscript. Each author contributed to the research as follows: M.G. was responsible for supervision, conceptualization, methodology, investigation, validation, formal analysis, resources, visualization, writing –original draft, and project adminis-

tration; Farshid Soleimani contributed to the resources, and writing – review & editing; H.A. was contributed to writing – review & editing; S.G. was contributed to visualization . All authors reviewed the manuscript.

Declarations

Competing interests

The authors declare no competing interests.

Additional information

Supplementary Information The online version contains supplementary material available at <https://doi.org/10.1038/s41598-024-78198-5>.

Correspondence and requests for materials should be addressed to M.G.

Reprints and permissions information is available at www.nature.com/reprints.

Publisher's note Springer Nature remains neutral with regard to jurisdictional claims in published maps and institutional affiliations.

Open Access This article is licensed under a Creative Commons Attribution-NonCommercial-NoDerivatives 4.0 International License, which permits any non-commercial use, sharing, distribution and reproduction in any medium or format, as long as you give appropriate credit to the original author(s) and the source, provide a link to the Creative Commons licence, and indicate if you modified the licensed material. You do not have permission under this licence to share adapted material derived from this article or parts of it. The images or other third party material in this article are included in the article's Creative Commons licence, unless indicated otherwise in a credit line to the material. If material is not included in the article's Creative Commons licence and your intended use is not permitted by statutory regulation or exceeds the permitted use, you will need to obtain permission directly from the copyright holder. To view a copy of this licence, visit <http://creativecommons.org/licenses/by-nc-nd/4.0/>.

© The Author(s) 2024